Next-to-Leading QCD Effect on the Quark Compositeness Search at the LHC

Jun Gao, Chong Sheng Li, Jian Wang, Hua Xing Zhu, and C.-P. Yuan

Phys. Rev. Lett. **106**, 142001 — Published 4 April 2011

DOI: 10.1103/PhysRevLett.106.142001

Next-to-leading QCD effect to the quark compositeness search at the LHC

Jun Gao,[1] Chong Sheng Li,[1,*] Jian Wang,[1] Hua Xing Zhu,[1] and C.-P.Yuan[2,†]

[1]*Department of Physics and State Key Laboratory of Nuclear Physics and Technology, Peking University, Beijing 100871, China*
[2]*Department of Physics and Astronomy, Michigan State University, East Lansing, 48824, USA*

We present the exact next-to-leading order (NLO) QCD corrections to the dijet production induced by the quark contact interactions at the CERN Large Hadron Collider (LHC). We show that as compared to the exact calculation, the scaled NLO QCD prediction adopted by the ATLAS Collaboration has overestimated the new physics effect on some direct observables by more than 30% and renders a higher limit on the quark compositeness scale. The destructive contribution from the exact NLO correction will also lower the compositeness scale limit set by the CMS Collaboration.

The quark composite models have been studied extensively in the literature [1, 2]. It is assumed that quarks are composed of more fundamental particles with new strong interactions at a composite scale Λ, much greater than the quark masses. At energy well below Λ, quark contact interactions are induced by the underlying strong dynamics, and yield observable signals at hadron colliders. For example, the dijet production at the CERN Large Hadron Collider (LHC) could be largely modified. In the Standard Model (SM), the theory of Quantum Chromodynamics (QCD) predicts the jets in dijet events are preferably produced in large rapidity region, via small angle scatterings in t-channel processes. On the contrary, the dijet angular distribution induced by the quark contact interactions is expected to be more isotropic. The D0 and CDF Collaborations at the Fermilab Tevatron have set limits on the scale Λ based on their dijet data [3]. Recently, both the ATLAS and CMS collaborations have carried out similar analyses [4, 5] using the LHC dijet data with $\sqrt{s} = 7$ TeV, in proton-proton collisions, and an integrated luminosity of about 3 pb^{-1}. The observed limits for Λ at the 95% confidence level (CL) are 3.4 TeV and 4.0 TeV, respectively, which have already exceeded the previous limits. With more integrated luminosity collected, these limits will be further improved.

The limits on the composite scale Λ were obtained by comparing the experimental dijet data with various theory predictions, including the SM next-to-leading order (NLO) QCD corrections and contribution induced by the quark contact interactions which were handled differently in different experiments. While the CMS Collaboration included only the leading order (LO) contribution from the quark contact interactions [5], the D0, CDF and ATLAS Collaborations included the "scaled NLO QCD correction" which assumes the NLO correction (in terms of K-factors) to the dijet production from the contact interactions to be exactly the same as that from the SM QCD interactions [3, 4]. In this Letter, we present the exact NLO QCD correction to the dijet production induced by the quark contact interactions, and discuss its impact to the existing experimental limits set by both the ATLAS and CMS Collaborations.

To compare with the experimental analyses, we consider only the quark contact interactions that are the products of left-handed electroweak isoscalar quark currents which are assumed to be flavor-symmetric to avoid large flavor-changing neutral-current interactions [2]. The effective Lagrangian can be written as

$$\mathcal{L}_{NP} = \frac{1}{2\Lambda^2}(c_1 O_1 + c_2 O_2), \tag{1}$$

where c_1, c_2 are the Wilson coefficients, and O_1, O_2 are the color-singlet and color-octet operators given by

$$\begin{aligned} O_1 &= \delta_{ij}\delta_{kl}\left(\sum_{c=1}^{3}\bar{q}_{Lci}\gamma_\mu q_{Lcj}\sum_{d=1}^{3}\bar{q}_{Ldk}\gamma^\mu q_{Ldl}\right), \\ O_2 &= \mathrm{T}^a_{ij}\mathrm{T}^a_{kl}\left(\sum_{c=1}^{3}\bar{q}_{Lci}\gamma_\mu q_{Lcj}\sum_{d=1}^{3}\bar{q}_{Ldk}\gamma^\mu q_{Ldl}\right), \end{aligned} \tag{2}$$

in which c, d are the generation indices and i, j, k, l, a are the color indices, and T^a are the Gell-Mann matrices. The Wilson coefficients at the scale Λ are conventionally normalized to be $c_1(\Lambda) = 4\pi\cos\theta$, $c_2(\Lambda) = 4\pi\sin\theta$, with $0 \le \theta < 2\pi$. Notice that the above operators can also arise from the exchange of new heavy resonances in various new physics models, such as Z' models [6] and extra dimensions models [7]. Thus, our analyses are rather model independent and Λ can be identified as the effective new physics (NP) scale. When using the above operators to calculate an observable at a scale much lower than Λ, we have to consider the QCD running effects of the Wilson coefficients [8], which can be easily derived by solving the renormalization group equation using the one-loop anomalous dimension matrix of the operators, as following:

$$\begin{pmatrix} c_1(\mu_R) \\ c_2(\mu_R) \end{pmatrix} = \begin{pmatrix} \frac{N+1}{2N} & \frac{N-1}{2N} \\ 1 & -1 \end{pmatrix} \begin{pmatrix} b_1 r^{\frac{-3(N-1)}{N\beta_0}} \\ b_2 r^{\frac{3(N+1)}{N\beta_0}} \end{pmatrix}, \tag{3}$$

with $r = \alpha_s(\mu_R)/\alpha_s(\Lambda)$, and

$$b_1 = c_1(\Lambda) + \frac{C_F}{N+1}c_2(\Lambda),\ b_2 = c_1(\Lambda) - \frac{C_F}{N-1}c_2(\Lambda), \tag{4}$$

where $N = 3$ and $C_F = 4/3$ for QCD, $\beta_0 = (11N - 2n_f)/3$, and μ_R is the renormalization scale, $n_f = 5$

is the number of active quark flavors. In the studies of the ATLAS and CMS Collaborations, they focus on the color-singlet operator with destructive interference, which corresponds to $\theta = 0$ in our analyses. Below, we will first discuss this case, and then extend to more general cases with arbitrary θ values.

At the LO, there are several subprocesses which contribute to the dijet production at hadron colliders induced by the NP operators we considered, including

$$qq'(q) \to qq'(q),\ q\bar{q}' \to q\bar{q}',\ q\bar{q} \to q\bar{q}(q'\bar{q}'), \qquad (5)$$

where q, q' could be all the quarks except the top quark. The NP contributions included in our calculation consist of two parts, the NP squared terms and the interference terms between the NP and the SM QCD interactions, which yield different kinematic distributions. We carried out the NLO calculations in the Feynman-'t Hooft gauge with dimensional regularization (DR) scheme (with naive γ_5 prescription) [8] in $n = 4-2\epsilon$ dimensions to regularize all the divergences. Below, we only show the analytical results for the subprocess $q(p_1)q'(p_2) \to q(p_3)q'(p_4)$, since the similar results for other subprocesses can be obtained by crossing symmetry.

First, we define the following abbreviations for the color structures and the matrix element,

$$\begin{aligned} \mathcal{M}_0 &= \bar{u}_L(p_3)\gamma_\mu u_L(p_1)\bar{u}_L(p_4)\gamma^\mu u_L(p_2), \\ \mathcal{C}_1 &= \delta_{i_3 i_1}\delta_{i_4 i_2},\ \mathcal{C}_2 = \mathrm{T}^a_{i_3 i_1}\mathrm{T}^a_{i_4 i_2}, \end{aligned} \qquad (6)$$

where i_{1-4} are the color indices of the external quarks. The LO scattering amplitudes induced by the NP and the SM QCD interactions can be separately written as

$$\begin{aligned} i\mathcal{M}^{tree}_{NP} &= i\mathcal{M}_0(c_1\mathcal{C}_1 + c_2\mathcal{C}_2)/\Lambda^2, \\ i\mathcal{M}^{tree}_{SM} &= i\mathcal{M}_0(4\pi\alpha_s\mathcal{C}_2)/t, \end{aligned} \qquad (7)$$

where s, t, u are the Mandelstam variables, and we only keep the left-handed current product of the SM QCD amplitudes here since others have no interference with the NP interactions. After adding the 1-loop amplitudes and the corresponding counterterms, we have the ultraviolet finite virtual amplitudes as follows.

$$\begin{aligned} i\mathcal{M}^{v}_{NP} &= i\mathcal{M}_0 C_\epsilon \frac{\alpha_s}{4\pi}\Big\{ -2C_F\Big[c_1\mathcal{A}(t) + \frac{c_2}{2N}\mathcal{B}(u)\Big]\mathcal{C}_1 \\ &+\Big[c_1\big(-2\mathcal{B}(u)\big) + c_2\big(-2C_F\mathcal{A}(u) + \frac{1}{N}\big(\mathcal{B}(u) + \\ &\mathcal{B}(t)\big)\big)\Big]\mathcal{C}_2\Big\}/\Lambda^2, \\ i\mathcal{M}^{v}_{SM} &= i\mathcal{M}_0 C_\epsilon \frac{\alpha_s}{4\pi}\Big\{4\pi\alpha_s\Big[-\frac{C_F}{2N}\Big(\frac{4}{\epsilon}\ln(-\frac{s}{u}) - \\ &2\frac{t}{s}\ln(\frac{t}{u}) - \frac{u^2}{s^2}\ln^2(\frac{t}{u}) + \ln^2(\frac{s^2}{tu}) + (1-\frac{u^2}{s^2})\pi^2\Big)\Big] \\ &\mathcal{C}_1 + 4\pi\alpha_s\Big[-2C_F\Big(\frac{2}{\epsilon^2} + \frac{1}{\epsilon}\big(3 + 2\ln(-\frac{s}{u})\big)\Big) \\ &+\frac{2}{N\epsilon}\ln(\frac{s^2}{tu}) + \beta_0\ln(\frac{\mu_R^2}{s}) - (\frac{2}{3}n_f - \frac{10}{3}C_F - \frac{8}{3N}) \\ &\ln(-\frac{s}{t}) + \frac{3}{N}\ln^2(-\frac{s}{t}) - \big(\frac{1}{2N} - C_F\big)\Big(\frac{u^2}{s^2}\big(\ln^2(\frac{t}{u}) \\ &+\pi^2\big) - 2\frac{u}{s}\ln(\frac{t}{u}) + \ln^2(\frac{t}{u}) - 2\ln(-\frac{s}{u})\big(1 + \\ &\ln(-\frac{s}{u})\big)\Big) + \big(C_F + \frac{3}{2N}\big)\pi^2 - \big(\frac{10}{9}n_f - \frac{26}{9}C_F \\ &-\frac{85}{9N}\big)\Big]\mathcal{C}_2\Big\}/t, \end{aligned} \qquad (8)$$

where $C_\epsilon = (\frac{4\pi\mu_R^2}{s})^\epsilon \frac{1}{\Gamma(1-\epsilon)}$, and

$$\begin{aligned} \mathcal{B}(x) &= \frac{2}{\epsilon}\ln(-\frac{s}{x}) + 3\ln(-\frac{\mu_R^2}{x}) + \ln^2(-\frac{s}{x}) + \pi^2 + 9, \\ \mathcal{A}(x) &= \frac{2}{\epsilon^2} + \frac{3}{\epsilon} + (\frac{2}{\epsilon} + 3)\ln(-\frac{s}{x}) + \ln^2(-\frac{s}{x}) + 8. \end{aligned} \qquad (9)$$

We have checked that the virtual correction for the SM QCD contributions given in Eq. (8) agrees with the ones shown in Ref. [9]. The infrared divergences in virtual corrections should cancel with those in real corrections. As for the real corrections, we apply both the two cutoff method [10] and the dipole subtraction method [11] in our calculations for a cross-check, and will present the details elsewhere due to the limited space.

To compare with the dijet measurements of the ATLAS and CMS, we adopt the anti-k_T jet algorithm [12] with the E_T recombination scheme [13] at parton level. We use the same parton distribution function sets [14] and set both the renormalization and factorization scales to the average jet transverse momentum p_T, as in the experimental analyses. Since our calculations are based on the effective field theory approach, we only consider the dijet invariant mas m_{jj} up to the NP scale Λ. The SM QCD contributions are also calculated up to NLO, using both the modified EKS code [15] and the NLOjet++ program [16] for a cross-check.

The ATLAS measurement — Following the ATLAS analysis, we impose the following kinematic cuts for selecting the dijet events.

$$\begin{aligned} &|y_{jet}| < 2.8,\ p_{T1(2)} > 60(30)\mathrm{GeV},\ m_{jj} > 1.2\mathrm{TeV}, \\ &|y_b| = |y_1 + y_2|/2 < 0.75,\ |y^*| = |y_1 - y_2|/2 < 1.7. \end{aligned} \qquad (10)$$

The jet radius parameter ΔR is chosen to be 0.6. We note that at parton level, the constraints on y^* and m_{jj} have already set a threshold of about 150 GeV for p_{T2}. To quantify the NP effects on dijet angular distribution, we divide the region of $|y^*|$, between 0 and 3.3/2, into 11 bins with equal bin width, and define F as the ratio of the number of events in the first 4 bins (with cross section $\sigma(4th)$) to that in the total 11 bins (with cross section $\sigma(tot)$) [4]. In Fig. 1(a) we show the effect of new physics contribution, defined through the discriminator $\Delta = (F_{NP+SM} - F_{SM})/F_{SM}$, i.e.,

$$\Delta = \frac{F_{NP+SM}}{F_{SM}} - 1 = \frac{\sigma_{NP+SM}(4th)/\sigma_{SM}(4th)}{\sigma_{NP+SM}(tot)/\sigma_{SM}(tot)} - 1, \qquad (11)$$

as a function of the compositeness scale Λ in three cases: (1) including only the LO results as done by CMS; (2) using the scaled NLO QCD results as done by ATLAS; (3) including the exact NLO QCD corrections presented in this Letter. While the scaled NLO QCD calculation predicts a higher value of Δ than the LO calculation, the exact NLO QCD calculation yields a much smaller value. To further quantify the differences, we plot in Fig. 2 the ratios (K-factors) of the scaled NLO (labeled as NLO1) and the exact NLO (labeled as NLO2) predictions for Δ to the LO results as functions of Λ. The difference in the two NLO K-factors is also shown, which is generally larger than 30% for Λ larger than about 3 TeV. Using the scaled NLO prediction, ATLAS found the 95% CL exclusion limit on the quark compositeness scale is 3.4 TeV, which corresponds to Δ value about 0.38. If using the exact NLO QCD calculation, the exclusion limit will reduce by about 10% to 3.1 TeV.

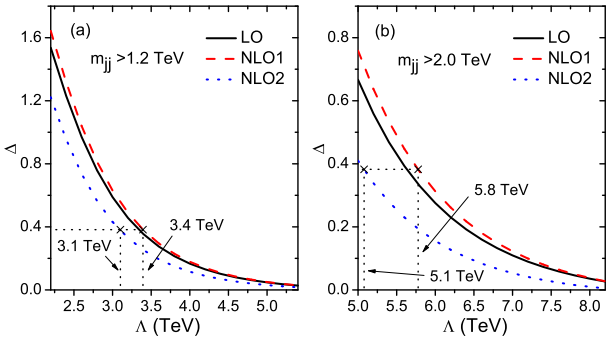

FIG. 1: Δ as functions of the scale Λ. The NLO1 (2) curves represent the scaled (exact) NLO results.

Fig. 1(b) shows similar results as Fig. 1(a), but requiring the dijet invariant mass to be larger than 2 TeV instead of 1.2 TeV. This measurement will become feasible when more integrated luminosity is collected at the LHC. Again, the scaled NLO calculation would overestimate the exclusion limit as compared to the exact NLO QCD calculation. For $\Delta = 0.38$, the difference is more than 10%.

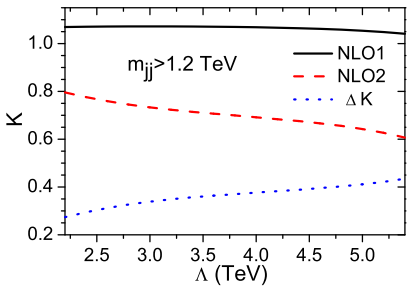

FIG. 2: The scaled NLO and the exact NLO K-factors, and their differences, as functions of Λ.

The CMS measurement — Following the CMS analyses, we require

$$|\eta_{jet}| < 1.3,\ p_{Tjet} > 50\text{GeV},\ \Delta R = 0.7, \qquad (12)$$

and define the centrality ratio R^η as the number of events in the inner pseudo-rapidity region $|\eta_{1,2}| < 0.7$ (with cross section σ_{in}) to the one in the outer region $0.7 < |\eta_{1,2}| < 1.3$ (with cross section σ_{out}) to quantify the NP effects on the dijet angular distribution, and evaluate R^η in each invariant mass bin from several hundred GeV to 3 TeV [5]. In our calculation we use the same cuts and strategy as the CMS except that we only consider the last five invariant mass bins with equal width ranging from 1.5 TeV to 3 TeV, since the NP effects are more significant in this region. To quantitatively compare various theory predictions, we introduce the discriminator ρ as the weighted average deviation of R^η from the SM predictions,

$$\rho = \Big(\sum_{i=1}^{5} \omega_i \big|R^\eta_{NP+SM}(i) - R^\eta_{SM}(i)\big|/R^\eta_{SM}(i)\Big) \Big/ \sum_{i=1}^{5} \omega_i,$$
$$\omega_i = \sqrt{\mathcal{L}/\big(\sigma_{in,NP+SM}(i)^{-1} + \sigma_{out,NP+SM}(i)^{-1}\big)}, \qquad (13)$$

where ω_i is the inverse of the relative statistical error of $R^\eta_{NP+SM}(i)$, and $\mathcal{L}$ is the integrated luminosity. In Fig. 3(a), we plot ρ as functions of the compositeness scale Λ, as predicted by the LO and the exact NLO calculations. The exact NLO QCD corrections generally reduce the value of ρ as compared to the LO prediction. For completeness, the exact NLO K-factors of ρ are shown in Fig. 3(b). Consequently, the exact NLO QCD corrections modify the CMS 95% CL exclusion limit of Λ from 4.0 TeV to 3.7 TeV.

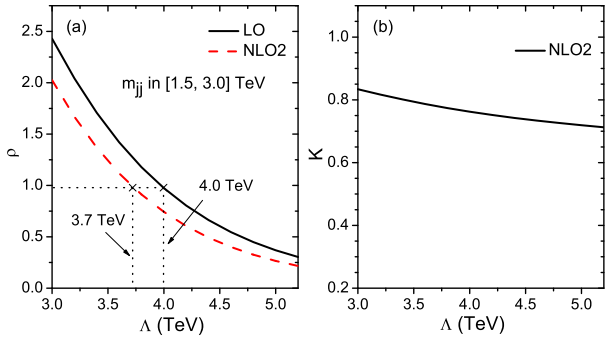

FIG. 3: (a) ρ as functions of the compositeness scale Λ, as predicted by the LO and the exact NLO calculations. (b) The exact NLO K-factors of ρ, as functions of Λ.

General cases with arbitrary θ values — It is interesting to also study the general cases in which both the $c_1(\Lambda)$ and $c_2(\Lambda)$ coefficients in the effective Lagrangian are nonzero. Here, we consider the discovery potential of the LHC with $\sqrt{s} = 14$ TeV, and raise the dijet invariant mass cut to 3 TeV. In Fig. 4 we plot the discriminator Δ

as functions of θ for different values of Λ together with the 3σ error bands from the SM predictions, which are calculated by assuming an integrated luminosity of 1 fb^{-1}. We find that Δ varies largely from positive to negative values with the change of θ for a given Λ value, and the difference between the scaled NLO and the exact NLO predictions can be larger than 30%. Another interesting observation is that there are regions of theory parameter space in which the NP effects on the angular distribution vanish, due to the cancellation of the contributions from the O_1 and O_2 operators. In that case, it will be difficult to study the quark compositeness scale through the dijet angular distribution measurement at the LHC. Finally, the quark contact interactions can also modify the top quark pair production at the Tevatron and the LHC. It may be possible to distinguish the effects induced from the two operators by studying the correlations between the dijet and the top quark pair production processes, which will be presented elsewhere.

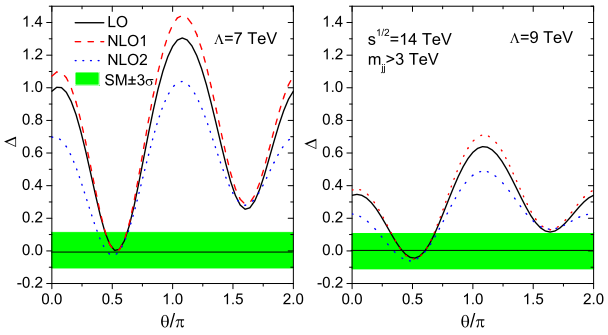

FIG. 4: Δ as functions of θ for different values of Λ.

In conclusion, we have calculated the exact NLO QCD corrections to the dijet production at the LHC, induced by the quark contact interactions which may arise from the quark compositeness models or other new physics models. From our results, the current exclusion limits of the quark compositeness scale set by the ATLAS and CMS Collaborations shall be lowered from 3.4 TeV to 3.1 TeV, and 4.0 TeV to 3.7 TeV, respectively. Moreover, we discussed the general cases with color-octet operator included in the quark contact interactions and found that in some regions of the theory parameter space, the quark compositeness may become undetectable at the LHC via the dijet angular distribution measurement.

This work was supported in part by the National Natural Science Foundation of China, under Grants No.11021092 and No.10975004. C.P.Y acknowledges the support of the U.S. National Science Foundation under Grand No. PHY-0855561.

* Electronic address: csli@pku.edu.cn
† Electronic address: yuan@pa.msu.edu

[1] E. Eichten, K. D. Lane and M. E. Peskin, Phys. Rev. Lett. **50**, 811 (1983); E. Eichten, I. Hinchliffe, K. D. Lane and C. Quigg, Rev. Mod. Phys. **56**, 579 (1984) [Addendum-ibid. **58**, 1065 (1986)]; P. Chiappetta and M. Perrottet, Phys. Lett. B **253**, 489 (1991).
[2] K. D. Lane, arXiv:hep-ph/9605257.
[3] F. Abe *et al.* [CDF Collaboration], Phys. Rev. Lett. **77**, 5336 (1996) [Erratum-ibid. **78**, 4307 (1997)]; T. Aaltonen *et al.* [CDF Collaboration], Phys. Rev. D **79**, 112002 (2009); V. M. Abazov *et al.* [D0 Collaboration], Phys. Rev. Lett. **103**, 191803 (2009).
[4] G. Aad *et al.* [ATLAS Collaboration], Phys. Lett. B **694**, 327 (2011).
[5] V. Khachatryan *et al.* [CMS Collaboration], Phys. Rev. Lett. **105**, 262001 (2010).
[6] P. Langacker, Rev. Mod. Phys. **81**, 1199 (2008).
[7] L. Randall and R. Sundrum, Phys. Rev. Lett. **83**, 3370 (1999) .
[8] G. Buchalla, A. J. Buras and M. E. Lautenbacher, Rev. Mod. Phys. **68**, 1125 (1996).
[9] R. K. Ellis and J. C. Sexton, Nucl. Phys. B **269**, 445 (1986).
[10] B. W. Harris and J. F. Owens, Phys. Rev. D **65**, 094032 (2002).
[11] S. Catani and M. H. Seymour, Nucl. Phys. B **485**, 291 (1997) [Erratum-ibid. B **510**, 503 (1998)].
[12] M. Cacciari, G. P. Salam and G. Soyez, JHEP **0804**, 063 (2008).
[13] G. L. Bayatian *et al.* [CMS Collaboration], CERN-LHCC-2006-001.
[14] J. Pumplin, D. R. Stump, J. Huston, H. L. Lai, P. M. Nadolsky and W. K. Tung, JHEP **0207**, 012 (2002); A. Sherstnev and R. S. Thorne, Eur. Phys. J. C **55**, 553 (2008); P. M. Nadolsky *et al.*, Phys. Rev. D **78**, 013004 (2008).
[15] S. D. Ellis, Z. Kunszt and D. E. Soper, Phys. Rev. Lett. **69**, 1496 (1992).
[16] Z. Nagy, Phys. Rev. Lett. **88**, 122003 (2002).